Solvent dynamical effects in electron transfer: molecular dynamics simulations of reactions in methanol

ARTICLE *in* CHEMICAL PHYSICS · OCTOBER 1993

Impact Factor: 1.65 · DOI: 10.1016/0301-0104(93)80262-8

3 AUTHORS, INCLUDING:

Donald K Phelps
Air Force Research Laboratory
30 PUBLICATIONS **490** CITATIONS
SEE PROFILE

Branka M. Ladanyi
Colorado State University
152 PUBLICATIONS **5,082** CITATIONS
SEE PROFILE

OFFICE OF NAVAL RESEARCH

Contract No. N00014-91-J-1409

Technical Report No. 139

Solvent Dynamical Effects in Electron Transfer: Molecular Dynamics Simulations of Reactions in Methanol

by

Donald K. Phelps, Michael J. Weaver, and Branka M. Ladanyi

Prepared for Publication

in

Chemical Physics

Department of Chemistry

Purdue University

West Lafayette, IN 47907-1393

April 1993

ABSTRACT

Molecular-dynamics simulations of activated electron-transfer (ET) reactions in methanol have been undertaken in order to explore the physical nature of the solvent dynamics coupled to ET barrier crossing, and to probe some underlying reasons for the facile kinetics observed in this solvent. The reactant is modeled by a pair of Lennard-Jones (LJ) spheres in contact, of varying diameter (4 or 5 Å), and containing a univalent charge (cation or anion) on one site so to probe possible effects of the ionic charge sign. Following equilibration, the collective solvent response to a sudden charge transfer between the spherical sites is followed, and described in terms of the response function C(t), describing the difference in the solvent-induced electrostatic potential between the initial and final solute states. In all cases, the C(t) curves exhibit a very rapid (50-100 fs) initial decay component associated with hydroxyl inertial motion, followed by components arising from hydrogen-bond librational and diffusive motions. Interestingly, the dynamics and relative importance of these relaxation modes are dependent on the charge sign as well as size of the solute pair. The molecular-level origins of these sensitivities are explored by examining time-dependent radial distribution functions, which implicate the dominance of short-range solvation in the rapid relaxation dynamics. In particular, the initial very rapid C(t) component for the smaller anion-neutral reactant pair is seen to arise chiefly from dissipation of the hydroxyl solvent polarization around the newly formed neutral site following ET, being accompanied by a slower build up of solvent structuring around the adjacent anionic site. The simulated ET reorganization energies are also shown to be dependent upon the reactant size and charge type. Some more general implications of these and other MD simulation results to the elucidation of dynamical solvent effects in activated ET processes are also noted.

INTRODUCTION

Rates of chemical reactions involving charge redistribution are often influenced strongly by polar solvents. Over the past decade there has been a rapid development in our theoretical and experimental understanding of the role of solvent dynamics on such reaction rates. These studies have been concerned with time-dependent fluorescence Stokes shifts (TDFS), ionic and dipolar solvation dynamics[1-6], and, of particular interest to us here, activated electron-transfer (ET) reactions[7,8]. Progress in these closely related areas has been the subject of a number of informed review articles, including those cited above. The dynamics of solvent reorganization, which is expected to influence adiabatic ET rates, is linked intimately to the response of the solvent to an instantaneous change in the solute charge distribution observed in TDFS experiments.

While often beset with difficulties in separating contributions to the observed ET rates from dynamics and activation energetics, there is nevertheless firm experimental evidence that overdamped solvent relaxation can dominate the adiabatic barrier-crossing frequency, ν_n, in some cases[7,8]. The situation is apparently most straightforward in so-called Debye solvents, for which the uniform-phase dielectric relaxation is described approximately by a single exponential decay. For reactions in such media where the activation barrier is also associated chiefly with solvent reorganization, ν_n is found to correlate roughly with the inverse longitudinal relaxation time, τ_L^{-1}, as anticipated on the basis of the simple dielectric-continuum picture[8]. A notably different situation may apply at least to reaction dynamics in non-Debye liquids, especially alcohols, that feature additional shorter-time components in the dielectric loss spectrum. Barrier-crossing frequencies that are markedly

accelerated above τ_L^{-1} have been observed for a number of outer-sphere ET reactions in primary alcohols[9-16]. Part of the often large (~10 fold) rate accelerations can be accounted for[15] in terms of a continuum-based formulation due to Hynes[17]. A subsequent comparison between TDFS data obtained for coumarins and ET dynamics extracted from kinetic and optical data for metallocene self-exchanges highlights the importance of rapid (< 1 ps) solvent relaxation components to the barrier-crossing dynamics in methanol[7,16].

Such documented rate effects provide additional motivation for elucidating the molecular-level nature of the remarkably facile dynamics that are partly responsible for the ET reaction rates in this and other solvents. To this end, it is necessary to proceed beyond dielectric-continuum models in order to explore the role of short-range solvation in the reaction dynamics. Theoretical approaches to this problem have included the use of integral equation methods, such as the mean spherical approximation (MSA), and generalized continuum tactics which attempt to account for the wavevector (**k**)- as well as frequency-dependence of the solvent dielectric permittivity[3,4,18,19]. The former, however, suffer from an inadequate account of solvent-solvent interactions, while the latter face the difficulty of deducing suitable **k**-dependent dielectric parameters.

Recently, several authors have explored these and related solvation issues by means of molecular dynamics (MD) simulations[4,20-30]. While the simulated systems inevitably provide only incomplete models of the actual condensed-phase environment, they can aid considerably our appreciation of the *molecular-level* details of nonequilibrium as well as equilibrium solvation, and provide a critical test of analytic theories of solvation dynamics[4,5]. A significant common finding for the MD studies reported to date is that fast, non-diffusive, relaxation mechanisms, primarily inertial dynamics and, in hydrogen-bonding

solvents, librational dynamics as well, can constitute major contributors to the solvent response to charge transfer. Methanol is the only solvent studied so far for which these fast relaxation mechanisms do not dominate the solvation dynamics, with overdamped (diffusive) motion being an important additional contributor. The results of Fonseca and Ladanyi[20] on the relaxation of the methanol solvent in response to dipole creation in a diatomic solute differ from other MD results on solvation dynamics in another important respect: a significant departure of the nonequilibrium solvation response from the relaxation predicted by the linear-response (LR) approximation was found. Other MD studies found good agreement with LR for comparable magnitude of the change in solute-solvent interactions[4]. This breakdown of LR in methanol is apparently related to the fact that several relaxation timescales contribute importantly to the solvation dynamics[20]. Since this characteristic is shared by other alcohols as well as other non-Debye solvents, the validity of LR, which is commonly presumed in theoretical models of solvation dynamics, has been called into question.

The present paper reports MD simulations of intermolecular ET reactions in methanol, the reactant pair being modeled by a pair of juxtaposed spherical solutes, one charged and the other uncharged. The role of solute-solvent interactions is explored by altering both the solute size and univalent charge sign, thereby mimicking possible behavioral differences between the cation-neutral and anion-neutral reactant pairs which commonly constitute the self-exchange process utilized to probe solvent-dynamical effects[8]. The solvent reorganization dynamics coupled to the activated reaction are simulated by transferring an electron between the thermally equilibrated solute sites so to exchange the charge, and following the ensuing temporal changes in solvent

structure and energetics. This situation corresponds to that encountered experimentally in photoinduced electron transfer; there are nonetheless intrinsically close relationships between the dynamics and energetics of photoinduced and thermally activated ET processes. A similar MD simulation procedure was followed earlier by Chandler and coworkers in their examination of $Fe^{3+/2+}$ exchange in water[26]. It is nevertheless worth noting that the present MD–ET simulations differ from the majority of previous MD studies which are concerned with the formation (or annihilation) of a dipole from a neutral solute (or solute pair). The latter case refers specifically to TDFS and related ultrafast experimental probes of solvation dynamics. While inherently related, the effect of the net (unipolar) reactant charge upon the solvation dynamics and energetics, of central interest in intermolecular (and most intramolecular) ET systems, does not appear in the dipolar systems.

The present simulations reveal dynamics which uniformly contain contributions from three distinct relaxation mechanisms – inertial, hydrogen-bond librational, and diffusive motions. The relative contributions of these mechanisms to the overall dynamics vary according to the solute size and charge sign as well as timescale. The observed differences in the early-time dynamics are shown to be related to dissimilarities in the observed equilibrium-solvation structures; the variations in the dynamics of different-size anions can be rationalized further in terms of time-dependent radial distribution functions. We also test the linear-response approximation for charge transfer in methanol and find that it is not strictly valid. Finally, we comment upon the more general significance of the present findings to the molecular-level understanding of solvent dynamical effects in electron transfer.

MODELS AND METHODS

The model system used in our MD simulations consisted of 255 methanol molecules and one two-phase solute. Intermolecular interactions were represented as site-site Lennard-Jones (LJ) + Coulomb pair potentials, with parameters for the methanol and the solutes as given in Table I. The Lorentz-Berthelot combining rules $\sigma_{\alpha\beta} = (\sigma_\alpha + \sigma_\beta)/2$ and $\epsilon_{\alpha\beta} = (\epsilon_\alpha\epsilon_\beta)^{\frac{1}{2}}$ were used to obtain Lennard-Jones (LJ) diameters $\sigma_{\alpha\beta}$ and energies $\epsilon_{\alpha\beta}$ for interactions between pairs of unlike sites α and β. The model for methanol used in this work was developed by Haughney et al[31]; it is a rigid bond-length and bond-angle treatment in which the methyl (Me) group is represented by a single interaction center, and the other two sites are the oxygen (O) and hydroxyl hydrogen (H) atoms. The physical properties around room temperature[31-35], including the wavevector dielectric permittivity tensor[32] as well as some aspects of solvation dynamics[20] in this model solvent have previously been studied. The reactant partners are represented as a pair of spheres - one neutral, the other charged - both of which have the same mass and Lennard-Jones parameters ϵ_s and σ_s. The intersite distance is held fixed at σ_s, i.e., the two spheres are essentially in contact. Charge-transfer dynamics data were obtained for solutes of two different diameters (σ_s = 4 Å and 5 Å) and charges (+e and -e). (The examination of larger solutes in the present study was precluded by the markedly longer computational times arising from the greater number of solvent molecules that thereby need to be included.) In the remainder of this paper, these solutes will be referred to by their σ_s values and charge signs (e.g. 4 Å cation).

In the simulation, the 256 molecules were placed in a cubic box with sides of 25.9 Å length. Periodic boundary conditions and a spherical cut-off at one-half of the box length were applied to the Lennard-Jones interactions. A

modified version of the Ewald sum, which excludes contributions from solutes outside the central box, was used to treat long-range electrostatic interactions. The equations of motion were integrated using the Verlet leapfrog algorithm[36] and SHAKE[37] was utilized to maintain the bond length and angle constraints. The production runs were carried out in the NVE ensemble at an average temperature of 298 K, using 4 fs time steps.

Two types of MD simulation were performed. The response of the system to an instantaneous $(q,0) \rightarrow (0,q)$ electron transfer between the charged and the neutral solute site was simulated directly by nonequilibrium MD. In addition, MD trajectory data were generated to calculate the equilibrium solvent structure around the solutes and to obtain the linear-response approximation to the charge-transfer perturbation.

Each starting configuration for a nonequilibrium trajectory was generated from an initial equilibrated state by the following procedure. The charge on the solute was turned off so that the surrounding solvent was able to move about more freely than in the presence of a charged solute and the system was allowed to evolve for 250 time steps, each of 8 fs duration. The charge was then reinstated and the system allowed to come to equilibrium for 400 to 1400 additional 8 fs time steps. Finally, since the actual nonequilibrium trajectories were obtained using a 4 fs step size, each of the starting configurations obtained as described above, was equilibrated for an additional 20 steps, each of 4 fs duration. The temperature of the system remained stable, indicating that nothing unexpected happened as a result of the change of time step size. The equilibration times for different solute-solvent systems were not the same; the 5 Å cation and the 5 Å anion solutes were equilibrated for 400 time steps, the 4 Å cation for 600 time steps and the 4 Å anion for 1400 time steps. Longer equilibration times for

the smaller solutes and especially for the small anion system reflect the fact that a "tighter" solvation shell structure needs to be constructed after the ionic charge is generated, with accompanying slower dynamics (vide infra).

The response of the system to the (q,0) → (0,q) charge-transfer perturbation was observed for a period of 600 fs. At least 200 trajectories were averaged to obtain the response function of each solute. The quantity calculated in these nonequilibrium simulations is the response function

$$C(t) = [\overline{\Delta E(t)} - \overline{\Delta E(\infty)}]/[\overline{\Delta E(0)} - \overline{\Delta E(\infty)}] \qquad (1)$$

where $\Delta E = E_q - E_0$, E_q and E_0 are the electrostatic potentials due to the solvent at the charged (q) and neutral (0) solute sites, $t = 0$ is the time at which the charge-transfer perturbation is applied, $t = \infty$ corresponds to the equilibrated solute-solvent system, and the overbar denotes an average in the presence of the perturbation, i.e. over the nonequilibrium trajectories.

As noted below, comparison of the above response function, C(t), with the expectation of LR theory invites the calculation of the time-correlation function

$$\Delta(t) = \langle \delta\Delta E(t)\ \delta\Delta E(0) \rangle / \langle (\delta\Delta E)^2 \rangle \qquad (2)$$

where $\delta\Delta E(t) = \Delta E(t) - \langle \Delta E \rangle$ is the fluctuation in ΔE and $\langle \ldots \rangle$ denotes an equilibrium ensemble average. Because the two solute sites differ only in their charge and in view of the symmetry of the charge-transfer perturbation, $\overline{\Delta E(\infty)} = \langle \Delta E \rangle$ and $\overline{\Delta E(0)} = -\langle \Delta E \rangle$. For each solute-solvent system, the time correlation, $\Delta(t)$, was calculated from at least 5 equilibrium runs of 7500 4 fs steps. The starting points for these equilibrium runs were chosen from the starting configurations for the nonequilibrium trajectories, which were continued without applying the charge-transfer perturbation.

RESULTS AND DISCUSSION

The primary results of this work, the time (t) evolution of the nonequilibrium solute-solvent response functions, C(t), for the four solute cases considered here, 4 and 5 Å diameter spherical pairs containing univalent cations and anions, are presented in Figure 1. For clarity, the anion-response functions are offset by 0.2 upwards on the y-axis from the cation functions. All the C(t) curves exhibit hallmarks of three relaxation mechanisms: (1) Inertial dynamics, giving rise to a Gaussian decay at short times; (2) hydrogen-bond librations, commencing at intermediate times, after the initial inertial component; (3) strongly overdamped (diffusional) relaxation at longer times. The presence and characteristics of these relaxation modes were sketched by Fonseca and Ladanyi in their MD simulation of dipole creation in methanol[20]. These are also evident in dipolar relaxation of pure methanol solvent as observed in recent far-infrared absorption experiments[38] and in MD simulations[35]. The same relaxation mechanisms contribute to solvation dynamics in water[22,26,27], but there diffusional relaxation apparently plays a much less important role[20].

Interestingly, the relative contributions of these different relaxation mechanisms for the present ET systems are seen to differ according to the solute size and charge sign (Figure 1). Anticipating a similarity in the longer-time relaxation rate for all solutes, the overall solvent relaxation time is shorter for cations, more noticeably for the smaller solutes, than for anions despite the fact that the initial inertial-driven decay is more rapid for the latter. These differences in C(t) for ions of the same charge and different size are significant, but do not exhibit a simple trend: faster relaxation rates are observed for smaller cations and larger anions. In broad outline, these C(t) traces are reminiscent of the MD simulations obtained for dipole creation in

methanol by Fonseca and Ladanyi[20]. As might be expected, the latter C(t) responses appear to lie somewhat in between the C(t) curves for the cation and anion systems. The present data, however, show the presence of a more rapid overall decay to lower C(t) values (< 0.4-0.5), especially for the smaller cation reactant.

For ion-neutral solute pairs of the same size, the nature of simple ion-dipole solute-solvent interactions should be independent of the sign of the ionic charge. Consequently, the observed differences in the present simulations signal the importance of more involved solute-solvent interactions, manifesting themselves in the structure (i.e. molecular orientation, etc.) of the first one or two solvation shells and in the rearrangement dynamics within these shells in response to the electron transfer. In order to gain a more specific molecular-level understanding of the nature of the C(t) relaxations and their dependencies on solute size and charge sign, it is therefore instructive to inspect the temporal evolution of the radial distribution functions following electron transfer, as also can be provided by the MD simulations.

The various site-site radial distribution functions, g(r), for the H, O, and Me sites of methanol solvating the 4 Å charged solute spheres (cation or anion, as indicated) under equilibrium conditions are plotted in Figure 2A; the corresponding data for the 5 Å ions are shown in Figure 2B. Figure 3A provides similar distribution functions for the 4 Å cation and anion, but now measured from the center of the *uncharged* reactant partner within the charged-neutral reactant pair. Figure 3B contains corresponding information for the 5 Å solutes.

The most striking aspect of Figure 2 is the large difference in the degree of solvent structuring around the cations and anions. Because the hydroxyl hydrogen has no LJ potential and carries a substantial charge (0.43e),

equilibrium structures yielding a close proximity between H and the anion solute are strongly favored, resulting in a relatively ordered solvent environment (Figure 2). In the case of cations, the attractive coulombic interaction involves the methanol oxygen, for which the distance of closest approach is significantly larger due to LJ repulsion, so that the solvent structuring is more diffuse. As might be expected from the C(t) data, the location of the nearest-neighbor g(r) peaks are also dependent upon the ion size. For the cations, the stronger coulombic attraction yields a higher and narrower first oxygen g(r) peak, g_{-O}, surrounding the 4 Å ion, but the solvent structure around the 4 and 5 Å ions is otherwise quite similar. In contrast, the anionic solutes display a marked sensitivity of the g(r) solvent structure to the ion size. For the 4 Å ions, the nearest-neighbor -H peak is very high and sharp, indicating the predominance of oriented methanols with the hydroxyl H pointing towards the ion and the O and Me sites away from it. In the case of 5 Å anions, however, other structures are also quite likely, as can be deduced from the relatively sharp *second* g_{-H} and g_{-O} peaks and from the fact that the first g_{-Me} peak is higher than the first g_{-H} peak. This is indicative of structures in which the methyl group orients preferentially towards the ion, with the hydroxyl hydrogen positioned either towards or away from the charge. The latter structure allows hydrogen bonding between solvent molecules in the first and second solvation shells, leading to more favorable solvent-solvent interactions.

As expected, the solvent ordering around the adjacent neutral site is less sensitive to the solute size and the charge sign of the adjacent ionic site (Figure 3). The neutral site is seen to interact most favorably with the methyl group, which has the largest LJ energy and the smallest charge. Thus the first-neighbor Me peak is uniformly the largest and in the case of the 5 Å solutes, at

the shortest intersite distance. For the 5 Å solutes, the structure around the neutral is largely uninfluenced by the charge sign of the juxtaposed ionic solute (Figure 3B). Some effects of the presence of the adjacent ion, however, are seen for the 4 Å solutes (Figure 3A). They are weak for the O and Me centers, but the H distribution favors considerably shorter intersite separation when the neutral is adjacent to the anion. This is consistent with the fact that a short hydrogen-solute distance is strongly favored for the neighboring anion.

These variations in the local equilibrium solvation for differing solute pairs can help rationalize some of the aforementioned differences in the early-time dynamics following electron transfer (Figure 1). In all cases, the inertial component is due primarily to the motion of free hydroxyl hydrogens[20]. Immediately after the electron transfer, the density of hydroxyl hydrogens is the largest in the vicinity of the newly formed neutral site of the 4 Å anionic solute. These hydrogens are free to rotate around the methanol C–O bonds, giving rise to the larger initial decay component of C(t) for the smaller anionic solute (Figure 1). Hydrogen-bond libration, which corresponds to frustrated (i.e. non-free) rotation of the hydroxyl, plays a more important role for cations at early times, because the hydrogens in the first solvation shell are repelled by the ion and are more likely to form bonds to the more distant solvent molecules. This coupling to the solvent hydrogen-bond network is initially stronger for 5 Å versus 4 Å cations, accounting for the earlier and larger-amplitude librational oscillation for the larger ion (Figure 1).

While the equilibrium structures around the two solute sites can help understand some aspects of the dynamics, they are less useful at intermediate times, where nonequilibrium (time-dependent) structural information is more pertinent. In this latter time regime, a significant difference is observed in

the solvent relaxation rate for the 4 and 5 Å anions, but less so for the corresponding cations (Figure 1). We therefore concentrate on the former in the impending discussion. Figure 1 shows that the response function for the 4 Å anion decays rapidly up to about 80 fs, exhibits a slower relaxation rate to 200 fs, and then accelerates [relative to the corresponding C(t) for the 5 Å anion] during the next 150 fs. It is of particular interest to unravel the molecular-level factors responsible for such complex C(t) behavior.

A useful pictorial means of displaying information pertinent to this issue is in the form of radial distribution functions surrounding both solute sites gathered as a function of time following electron transfer. Figures 4A and B show such data for the hydroxyl hydrogen surrounding the 4 Å anion–neutral pair for the indicated series of time periods after electron transfer; A and B refer to the functions for the newly created anion and neutral sites, respectively. [Note that the initial, $t = 0$, $g(r)$ functions are omitted from the bottom of Figures 4A and B since these are identical to the equilibrium ($t = \infty$) functions also given in these figures; thus the $t = 0$ function for the newly formed neutral site is identical to the $t = \infty$ function for the anion site (Figure 4A), and vice versa.] Except for the $t = \infty$ data which were obtained from equilibrium simulations, these quantities were extracted from nonequilibrium trajectory data. Due to the statistical limitations, each nonequilibrium trace refers to an appropriately short (28 fs) time interval.

Inspection of Figure 4A shows that the sharp pronounced $g_{-H}(r)$ maximum at about $r = 2.3$ Å is developed substantially only for $t \gtrsim 200$ fs around the newly formed anion. Comparison of the $t = \infty$ trace in Figure 4A with the early-time curves in Figure 4B shows that the hydroxyl H structuring around the newly formed neutral site is attenuated severely even for $t \sim 80$ fs, the $g(r)$ traces

exhibiting only a diffuse broad structure throughout the later times. The form of the corresponding hydroxyl oxygen g(r) traces largely mirrors this behavior, although the changes are less marked at early times.

One can therefore identify, at least qualitatively, the origins of the C(t) morphology for the 4 Å anion system. The initial facile C(t) decay to about 80 fs is associated primarily with rapid destruction of the polarized solvent structure around the newly formed neutral site, whereas the ensuing slower relaxation arises chiefly from solvent structure developing around the newly formed anionic center. The shorter timescale for dissipating, as opposed to creating, the polarized solvation sphere may be rationalized on the basis of the anticipated case of dissociating a relatively ordered solvent structure as compared to forming it, i.e. on entropic grounds.

Such time-dependent g(r) curves can also account in broad terms for the markedly different C(t) morphologies seen for the 5 Å versus the 4 Å anion systems (Figure 1). Figures 5A and B contain analogous data as in Figures 4A and B, for the newly anionic and neutral sites, respectively, but for 5 Å solutes. As will be anticipated from the prior discussion, the temporal changes in solvent polarization are distinctively milder for the 5 Å as compared with the 4 Å solute. Thus although the short ($\lesssim$ 100 fs) and longer-time segments of the C(t) trace for the 5 Å solute can again be identified chiefly with structural changes surrounding the newly formed neutral and anionic solute, respectively, the temporal variations in g(r) are distinctly milder. In particular, this behavior accounts in simple fashion for the slower C(t) decay for the 5 Å versus 4 Å anion for $t > 200$ fs (Figure 1). Thus comparison of Figures 5A and 4A shows that the relative development of the $g_{-B}(r)$ maximum centered at ca 2.3 Å and 2.9 Å for the 4 Å and 5 Å anions, respectively, in the time regime 200-600 fs is significantly

less pronounced for the larger solute.

Some other interesting, although more subtle, pieces of molecular-level dynamical information can also be extracted from such temporal g(r) curves. For example, Figure 4 shows that significant polarization of the *second* solvation shell around the newly formed anion develops early - it is already reasonably well defined within the earliest time interval displayed (64-92 fs) - but that the first shell is still largely unstructured. The first solvation shell is formed subsequently, partially by removing molecules from the second shell, as deduced from the opposite temporal dependencies of the appropriate g(r) maxima (Figure 4A). It should be recognized, of course, that the quantitative link between the time-dependent g(r) traces and the overall response function is a complex one since the latter necessarily involves a detailed convolution of intermolecular forces. Nevertheless, such g(r) data can clearly provide some intriguing insight into the individual molecular motions responsible for the solvent dynamics.

Theoretical models for solvation dynamics usually assume that the linear response (LR) approximation applies to this process[4]. Fonseca and Ladanyi[20], however, have shown that this approximation is surprisingly poor for dipole creation in methanol. Here we test its validity for electron transfer in methanol. Figure 6 compares the time-evolution of corresponding C(t) and its LR counterpart, $\Delta(t)$, for 4 Å ions. Figure 7 is the counterpart of Figure 6 for 5 Å ions. Noticeable and even marked differences are seen between corresponding C(t) and $\Delta(t)$ traces, especially for the anionic systems and for the smaller (4 Å) solute. These disparities, which are generally diagnostic of a breakdown in the LR approximation[4,39], would appear to be associated with the specific solvation factors discussed above[20]. Interestingly, however, another common

hydrogen-bonded solvent, water, yields reasonable accordance to the LR approximation[22,26-28]. The LR approximation also holds for the ET energetics in water, a finding exemplified clearly in the near-perfect quadratic energy surface for the $Fe^{3+/2+}$ system as deduced from MD simulations[26]. The likely reasons for the marked behavioral difference between methanol and water have been discussed in ref. 20. All three moments of inertia of water are small and correspond primarily to hydroxyl hydrogen motion. Only one such moment of inertia is present in methanol. Thus fast inertial decay and O-H bond libration are much more efficient in relaxing the energy in water than in methanol.

In addition to solvation dynamics, the nonequilibrium MD simulations necessarily also provide information on the energetics of activated electron transfer[40]. Specifically, the $\langle \Delta E(\infty) \rangle$ values mentioned above equal the potential difference between the initial equilibrium and ET excited states, so that the quantity $|q\langle \Delta E(\infty) \rangle|$ can be identified with the so-called reorganization energy, λ, for electron transfer. Table II summarizes reorganization energies determined in this manner for the present systems in methanol, λ_{MD}. Listed underneath are the corresponding quantities, λ_{DC}, estimated from the conventional dielectric-continuum model due to Marcus[41]. (The latter was obtained from the usual two-sphere model, by setting the internuclear distance equal to twice the reactant radius.) Comparison of the corresponding λ_{MD} and λ_{DC} values reveals that they are in reasonable agreement for both the larger (5 Å) solutes and the smaller cation-neutral pair, yet the λ_{MD} value for the 4 Å anion-neutral reactant is markedly larger than λ_{DC}. Note that while the dielectric-continuum model necessarily predicts identical λ values for equal-sized anionic and cationic redox couples in a given solvent, only the λ_{MD} values for the larger solutes are comparable, the smaller anion solute yielding a λ_{MD} value that is about 40%

larger than for the cationic reactant (Table II).

This latter sensitivity of λ_{MD} to the charge sign of the ion-neutral reactant pair provides another manifestation of the differences in the short-range solvation of the anion and cation reactants discussed above. The larger λ_{MD} value for the 4 Å anion is unsurprising given the marked changes in short-range solvation attending electron transfer for this system, together with the breakdown in the LR approximation. Nevertheless, the nearly equal λ_{MD} values for the 5 Å cation and anion systems is more unexpected on this basis. Given that the LR approximation is noticeably less valid for the 5 Å anion than for the cation reactant (Figure 7, vide supra), the free energy-reaction coordinates should be decidedly nonparabolic, so that disparate λ_{MD} values might be expected for these systems. It is worth noting that the effective diameters of the majority of ET reactants commonly utilized to probe solvent dynamical effects are somewhat larger than 5 Å; for example, $\sigma \approx 7$-8 Å for simple metallocenes[9-11]. Consequently, the reasonable agreement between the λ_{MD} and λ_{DC} values observed for the 5 Å reactants (Table I) could be construed as lending support to the validity of the dielectric continuum model in this solvent.

Such agreement between λ_{MD} and λ_{DC} is, however, probably misleading. While the model for methanol used in the MD simulations accounts for the complex intermolecular forces involved in the solute-solvent interactions, it lacks a description of the electronic polarizability, instead tacitly setting the solvent optical dielectric constant, ϵ_{op}, equal to unity. It is well known that an important (or even predominant) contributor to the energetics of nonequilibrium solvent polarization, and hence to λ, is associated with the solvent electronic polarizability, as described by ϵ_{op} in the dielectric-continuum limit[41,42]. Since increasing the electronic polarizability stabilizes the ET transition

state, setting $\epsilon_{op} = 1$ should yield λ estimates that are too large. (The magnitude of the discrepancy should be roughly a factor of two in polar solvents, for which $\epsilon_{op} \sim 1.75$ to 2.4[42].) Inclusion of this factor should diminish λ_{MD} below the corresponding λ_{DC} estimates. Indeed, near-infrared optical measurements of λ, E_{op}, for mixed-valence ferrocenium-ferrocene systems in methanol yield values that are ca 20% below λ_{DC}, even though in most other polar solvents (with the notable exception of water) E_{op} is close to (within 5-10% of) λ_{DC}[43]. The origins of these disparities are unclear, but can be accounted for semiquantitatively by an "non-local" electrostatic treatment, whereby λ is diminished in such hydrogen-bound solvents by the reduced ability of the "structured" polarization to respond to local alterations in the electric field[44]. The solvent structuring effects observed in the present MD simulations have a rather different physical origin, arising from short-range solute-solvent interactions, and would appear to increase rather than diminish the ET barrier.

Implications For ET Solvent Dynamics

A clear feature that emerges from the present MD simulations, which is also seen in related dipole-creation and charge-transfer simulations in water[22,26-28] and acetonitrile[21], is the importance of a notably rapid inertial decay to the overall relaxation dynamics[4]. Indeed, a typical finding from the MD simulations in all three solvents is that the response function decays to below 0.5 in about 100 fs or less. In physical terms, then, a substantial relaxation of the excess energy present in the ET transition state, i.e. to energies markedly ($\gtrsim$ several k_BT) below the transition state in the products' well, can be accomplished extremely rapidly in these media. This rapid relaxation is seen to involve the first one or two solvation shells surrounding the solute. The observation of especially fast dynamics for short-range solvation differs from

the well-known Onsager "snowball" conjecture[45]. Slower relaxation dynamics for "close-in" solvent are also predicted by the nonequilibrium MSA treatment based on overdamped relaxation[46], and have been observed in MD simulations under similar conditions to the MSA model solvent[29]. Nevertheless, rapid short-time dynamics can be predicted under some conditions from analytic theory, as well as MD simulations, by considering partly inertial rather than purely overdamped motions[47].

Given that there is clear theoretical evidence that higher-frequency relaxations can dominate the ET barrier-crossing frequency, ν_n, when they make moderate or large contributions to the energetic response[15,17,48], one is tempted to assert that the reaction dynamics in experimental ET systems are at least partly controlled by such rapid inertial motions rather than the largely overdamped dynamics which are usually considered in discussions of ET kinetics[8]. Of course, as already mentioned, methanol is a "non-Debye" solvent, exhibiting at least one additional higher-frequency relaxation in the dielectric-loss spectrum[49]. This is apparently manifested as a rapid solvation relaxation component (τ_s ~ 1 ps) in ultrafast TDFS measurements reported by Barbara et al in methanol[16,50]. The high-frequency component observed in the present simulations in methanol, τ_s ~ 0.1 ps, is clearly much faster, occurring on a timescale below that readily accessible to TDFS experiments, and is not associated directly with the "non-Debye" properties of the pure methanol solvent. Nevertheless, the longer-time (i.e. slower) component of the C(t) traces in Figure 1 exhibits a relaxation time, ca 0.5 ps, which is compatible with the fast component observed in the Barbara et al measurements.*

* It is worth noting that the relaxation times provided by the present simulations are anticipated to be about twofold too short as a result of the neglect of the dielectric function of the solvent electronic polarizability to the overall longitudinal dynamics[4].

A key unresolved issue is the extent to which the remarkably rapid solvation dynamics as observed by MD simulations so far in water, acetonitrile, and methanol, are present in other media known (or at least anticipated) to offer higher solvent friction. The notably facile barrier-crossing frequencies for adiabatic electron-exchange processes involving suitable redox couples such as metallocenes in water, acetonitrile, and methanol[10,11,15,16] are certainly compatible with the involvement of such rapid MD relaxations, although the onset of nonadiabiticity anticipated towards higher frequencies may limit their importance except in ET processes featuring unusually strong donor-acceptor electronic coupling[16]. Slower ET reaction dynamics are observed in higher-friction solvents, such as benzonitrile and dimethylsulfide, so to yield solvent-dependent barrier-crossing frequencies varying in rough accordance with τ_L^{-1}, i.e. as expected from the overdamped dielectric-continuum treatment[7,8]. This finding by itself suggests, and has been commonly taken to indicate, that overdamped solvent relaxation plays a key role in controlling solvent dynamical effects on activated ET processes. However, in the light of the MD simulations, an alternative (albeit perhaps less palatable) interpretation is that the solvent-dependent ET dynamics are not described by continuum-like overdamped motion at all, but rather by the faster dynamics of short-range solvation *which may happen to correlate roughly with* τ_L^{-1}. Some related issues along these lines will be pursued elsewhere[51]. The exploration of this possibility would be one motivation for pursuing MD simulations, and also appropriate analytic theoretical treatments, in ostensibly higher-friction solvent media.

ACKNOWLEDGMENTS

We are most grateful to the late Teresa Fonseca for her central role in initiating this collaboration, even though she was not able to participate further in it. This work has been supported by grants from the Office of Naval Research (to MJW) and the National Science Foundation (to BML).

REFERENCES

[1] M. Maroncelli, J. MacInnis, and G.R. Fleming, Science. 243 (1989)1674.

[2] P.F. Barbara and W. Jarzeba, Adv. Photochem. 15 (1990) 1.

[3] B. Bagchi, Ann. Rev. Phys. Chem. 40 (1989) 115.

[4] M. Maroncelli, J. Mol. Liquids, perpetually in press.

[5] B.M. Ladanyi, Ann. Rev. Phys. Chem., in press.

[6] D.F. Calef, in "Photoinduced Electron Transfer", Part A, M.A. Fox, M. Chanon (eds), Elsevier, Amsterdam, 1988, page 362.

[7] M.J. Weaver and G.E. McManis, Acc. Chem. Res. 23 (1990) 294.

[8] M.J. Weaver, Chem. Rev. 92 (1992) 463.

[9] G.E. McManis, M.N. Golovin, and M.J. Weaver, J. Phys. Chem. 90 (1986) 6563.

[10] R.M. Nielson, G.E. McManis, and M.J. Weaver, J. Phys. Chem. 93 (1989) 4703.

[11] G.E. McManis, R.M. Nielson, A. Gochev, and M.J. Weaver, J. Am. Chem. Soc. 111 (1989) 5533.

[12] G. Grampp and W. Jaenike, Ber. Bensenges. Phys. Chem. 95 (1991) 904.

[13] M. Opallo, J. Chem. Soc. Faraday Trans. I 82 (1986) 339.

[14] D.K. Phelps, M.T. Ramm, Y. Wang, S.F. Nelsen, and M.J. Weaver, J. Phys. Chem. 97 (1993) 181.

[15] G.E. McManis and M.J. Weaver, J. Phys. Chem. 90 (1989) 912.

[16] M.J. Weaver, G.E. McManis, W. Jarzeba, and P.F. Barbara, J. Phys. Chem. 94 (1990) 1715.

[17] J.T. Hynes, J. Phys. Chem. 90 (1986) 3701.

[18] J.N. Onuchic and P.G, Wolynes, J. Phys. Chem. 92 (1988) 6495.

[19] B. Bagchi and G.R. Fleming, J. Phys. Chem. 94 (1990) 9.

[20] T. Fonseca and B.M. Ladanyi, J. Phys. Chem. 95 (1991) 2116.

[21] M. Maroncelli, J. Chem. Phys. 94 (1991) 2084.

[22] M. Maroncelli and G.R. Fleming, J. Chem. Phys. 89 (1988) 5044.

[23] P. VijayaKumar and B.L. Tembe, J. Chem. Phys. 95 (1991) 6430.

[24] E.A. Carter and J.T. Hynes, J. Phys. Chem. 93 (1989) 2184.

[25] D.A. Zichi, G. Ciccotti, J.T. Hynes, and M Ferrario, J. Phys. Chem. 93 (1989) 6261.

[26] (a) J.S. Bader and D. Chandler, Chem. Phys. Lett. 157 (1989) 501; (b) R.A. Kuharski, J.S. Bader, D. Chandler, M. Sprik, M.L. Klein and R.W. Impey, J. Chem. Phys., 89 (1988) 3248.

[27] (a) R.M. Levy, D.B. Kitchen, J.T. Blair, and K. Krogh-Jespersen, J. Phys. Chem 94 (1990) 4470; (b) M. Belhadj, D.B. Kitchen, K. Krogh-Jespersen, and R.M. Levy, J. Phys. Chem. 95 (1991) 1082.

[28] O.A. Karim, A.D.J. Haymet, M.J. Banet, and J.D. Simon, J. Phys. Chem. 92 (1988) 3391.

[29] L. Peters and M.L. Berkowicz, J. Chem. Phys. 96 (1992) 3092.

[30] A. Papazyan and M. Maroncelli, J. Chem. Phys. 95 (1991) 9219.

[31] M. Haughney, M. Ferrario and I.R. McDonald, J. Phys. Chem. 91 (1987) 4934.

[32] T. Fonseca and B.M. Ladanyi, J. Chem. Phys. 93 (1990) 8148.

[33] J. Alonso, F.J. Bermejo, M. Garcia-Hernanzex, J.L. Martinez, and W.S. Howells, J. Mol. Structure 200 (1991) 147.

[34] M. Matsumoto and K.E. Gubbins, J. Chem. Phys. 93 (1990) 1981.

[35] M. Skaf, T. Fonseca, and B.M. Ladanyi, J. Chem. Phys., in press.

[36] (a) L. Verlet, Phys. Rev. 159 (1967) 201; (b) M.P. Allen and D.J. Tildesley, Computer Simulation of Liquids (Oxford University Press, New York 1987) Ch. 3.

[37] G. Ciccotti and J.P. Ryckaert, Comput. Phys. Rep. 4 (1986) 345.

[38] B. Guillot, P. Marteau, and J. Obriot, J. Chem. Phys. 93 (1990) 6148.

[39] I. Rips and J. Jortner, J. Chem. Phys. 87 (1987) 2090.

[40] T. Fonseca, B.M. Ladanyi, and J.T. Hynes, J. Phys. Chem. 96 (1992) 4085.

[41] R.A. Marcus, J. Chem. Phys. 43 (1965) 679.

[42] For an explanative discussion, see: J.T. Hupp and M.J. Weaver, J. Phys. Chem. 89 (1985) 1601.

[43] G.E. McManis, A. Gochev, R.M. Nielsen and M.J. Weaver, J. Phys. Chem. 93 (1989) 7733.

[44] D.K. Phelps, A.A. Kornyshev and M.J. Weaver, J. Phys. Chem. 94 (1990) 1454.

[45] L. Onsager, Can. J. Chem. 55 (1977) 1819.

[46] P.G. Wolynes, J. Chem. Phys. 86 (1987) 5133.

[47] A. Chandra and B. Bagchi, Chem. Phys. 156 (1991) 323.

[48] T. Fonseca, J. Phys. Chem. 91 (1989) 2869.

[49] (a) J.A. Saxton, R.A. Bond, G.T. Coats, and R.M. Dickinson, J. Chem. Phys. 37 (1962) 2132; (b) G.H. Barbenza, Chem. Phys. 152 (1991) 57.

[50] W. Jarzeba, G.C. Walker, A.E. Johnson, and P.F. Barbara, Chem. Phys. 152 (1991) 57.

[51] M.J. Weaver, J. Mol. Liquids, in preparation.

TABLE I.

Potential Parameters for the Solvent and Solute

Solvent[a]

Site	q/e[b]	(ϵ/k_B)/K[c]	σ_S/Å[d]	mass/amu[e]
Me	0.297	91.2	3.861	15.024
O	−0.728	87.9	3.081	16.000
H	0.431	0	0	1.008

Solute[f]

Type	q/e[b]	$(\epsilon_S/Å)$/K[c]	σ/Å[d]	mass/amu[e]
4 Å cation	+1.0	150	4.0	60.0
4 Å anion	−1.0	150	5.0	60.0
5 Å cation	+1.0	150	4.0	60.0
5 Å anion	−1.0	150	5.0	60.0

a) geometry: R_{Me-O} = 1.43 Å; R_{O-H} = 0.945 Å; $Angle_{Me-O-H}$ = 108°53′.

b) Net charge on site indicated in left-hand column.

c) Lennard-Jones energy parameter.

d) Lennard-Jones diameter.

e) Site mass.

f) Solute is a pair of spheres at a center-to-center distance of σ_S, i.e. approximately in contact, one containing the charge as noted in left-hand column.

TABLE II.

Calculated Electron-Transfer Reorganization Energies (kcal mol^{-1})

Solute[a]	4 Å anion	4 Å cation	5 Å anion	5 Å cation
λ_{MD}[b]	58.6	42.5	30.2	31.4
λ_{DC}[c]	44.5	44.5	35.5	35.5

a) Solute is charged-neutral spherical pair in contact, with diameters as noted.

b) Reorganization energy as estimated by MD simulation (see text).

c) Reorganization energy as estimated from Marcus dielectric-continuum theory, using solvent parameters as in ref. 9.

FIGURE CAPTIONS

Figure 1

Response function, C(t), traces versus time following instantaneous symmetrical electron transfer within ion-neutral solute pairs in methanol. The full and dashed lines refer to 4 and 5 Å diameter solutes, respectively. Note that the traces for the anion-neutral pairs are offset by 0.2 upwards on the y-axis for clarity.

Figure 2

A) Equilibrium radial distribution functions for the H (full line), O (dashed line), and Me (dotted line) sites, as indicated, surrounding the charged sites in the 4 Å cation-neutral and anion-neutral sites (upper and lower panels, respectively).

B) As for A), but for 5 Å solutes.

Figure 3

A) As for Figure 2A, but for neutral 4 Å site.

B) As for Figure 2B, but for neutral 5 Å site.

Figure 4

A) Time-dependent radial distribution functions for hydroxyl H around newly created anion site following electron transfer in 4 Å anion-neutral solute. Traces corresponding to increasing times are offset progressively by 2.0 upwards along the y-axis.

B) As for A), but for newly formed neutral site.

Figure 5

A) As in Figure 4A, but for 5 Å anion site.

B) As in Figure 4B, but for 5 Å neutral site.

Figure 6

Comparison of the non-equilibrium response function C(t) and the corresponding time-correlation function Δ(t) vs time for 4 Å ion-neutral pairs in methanol. Anion-neutral curves (full lines); cation-neutral curves (dashed lines).

Figure 7

As for Figure 6, but for 5 Å ion-neutral solute pairs.

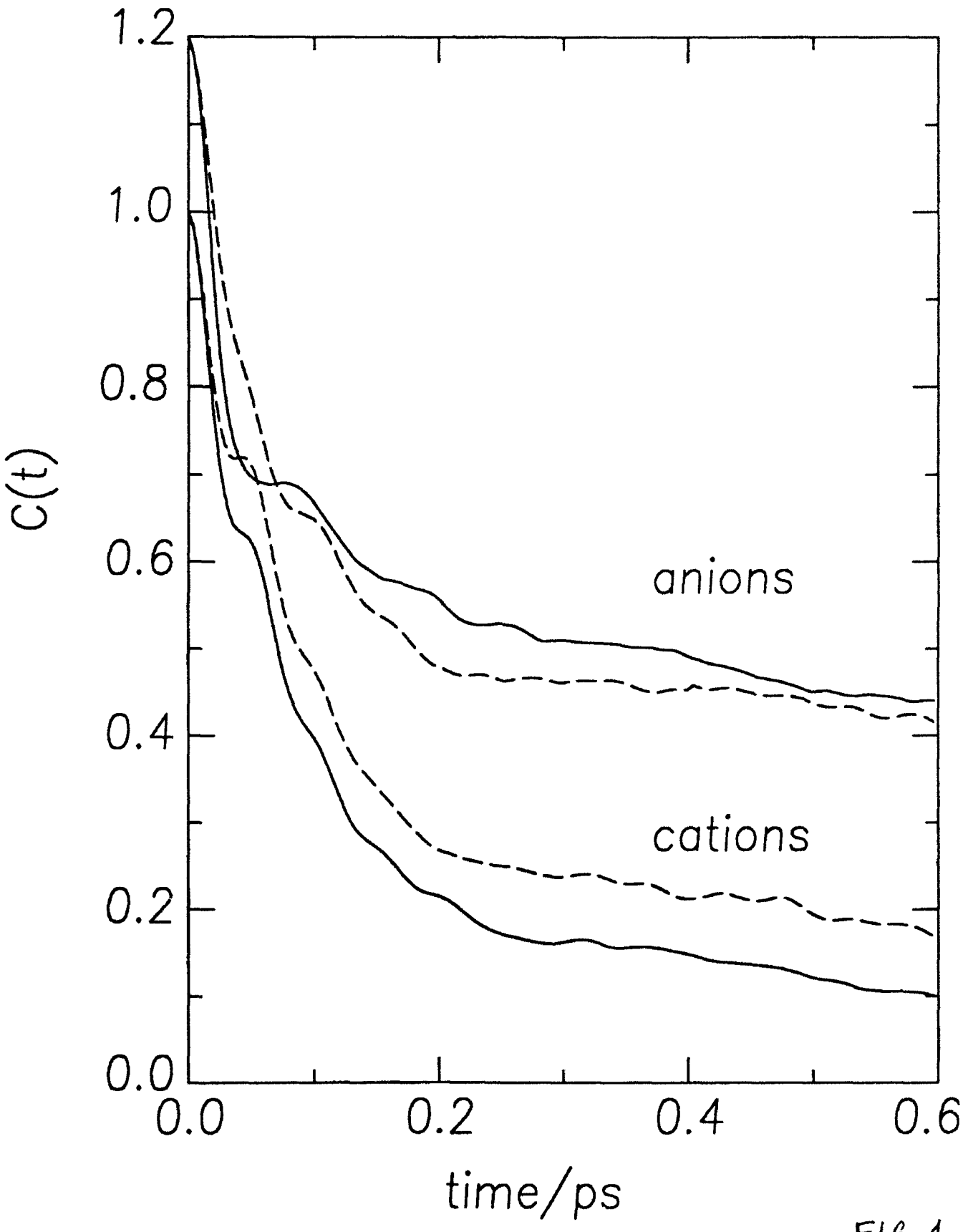

FIG 1

(A)

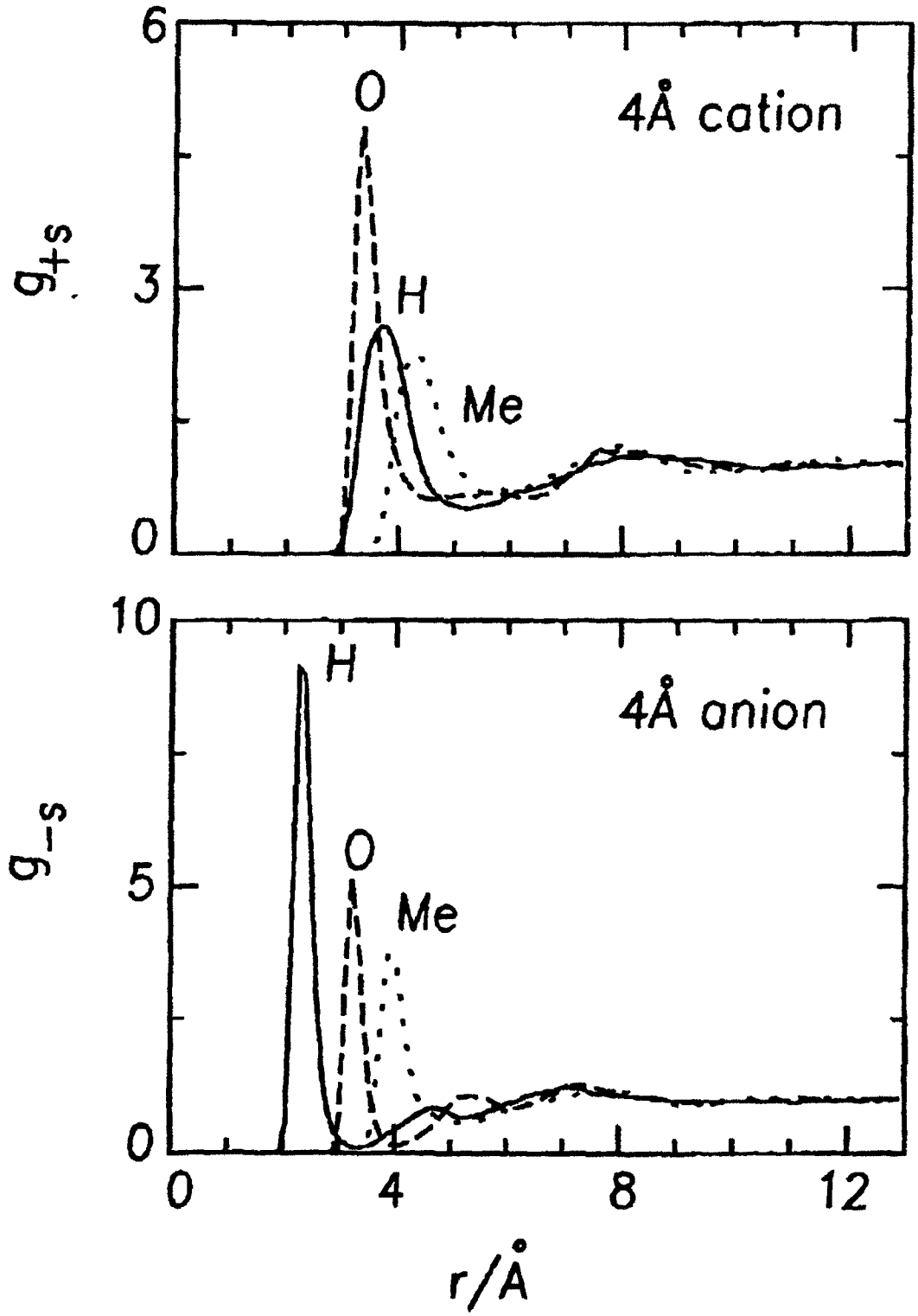

Fig. 2A

(B)

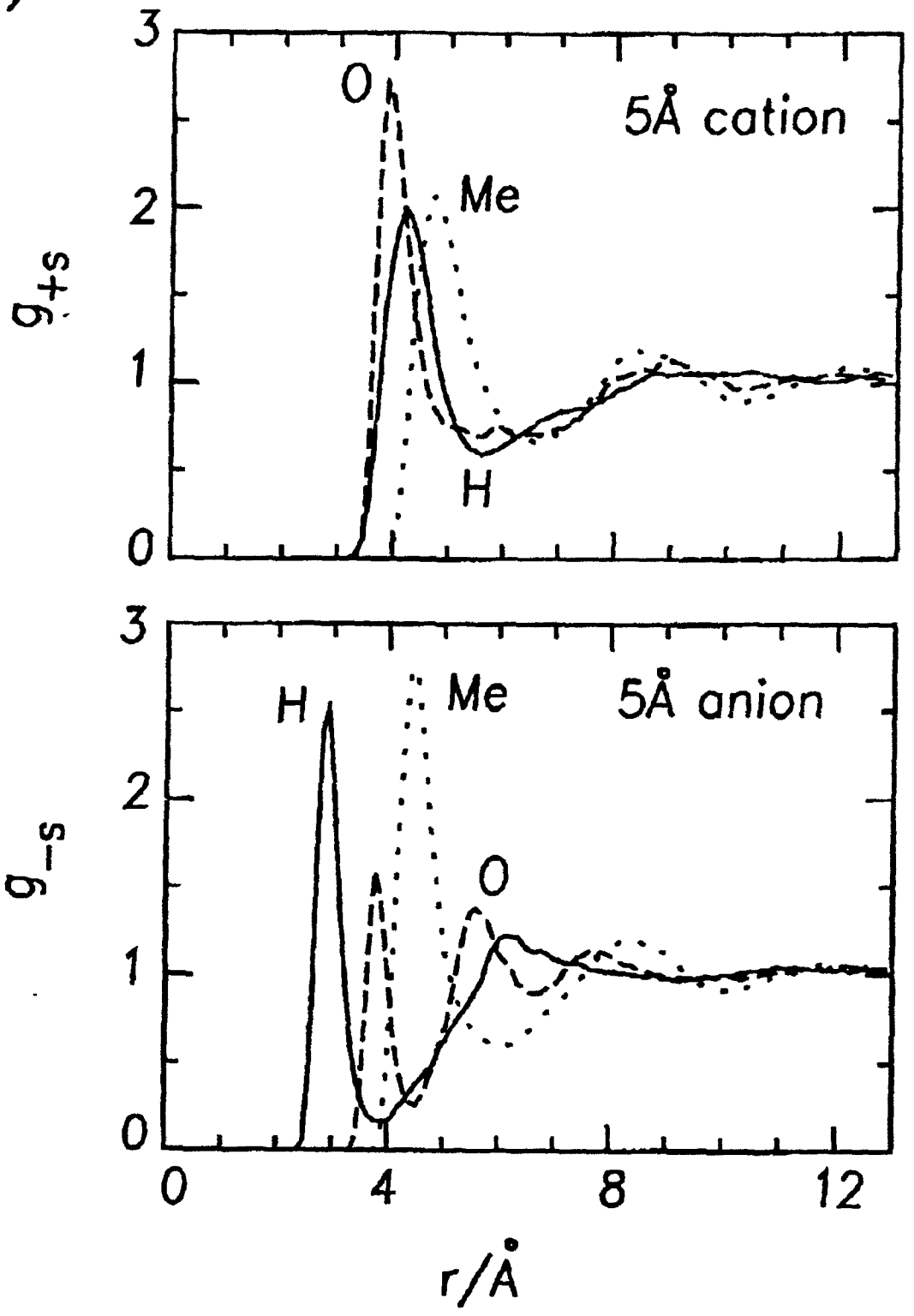

Fig. 2B

(A)

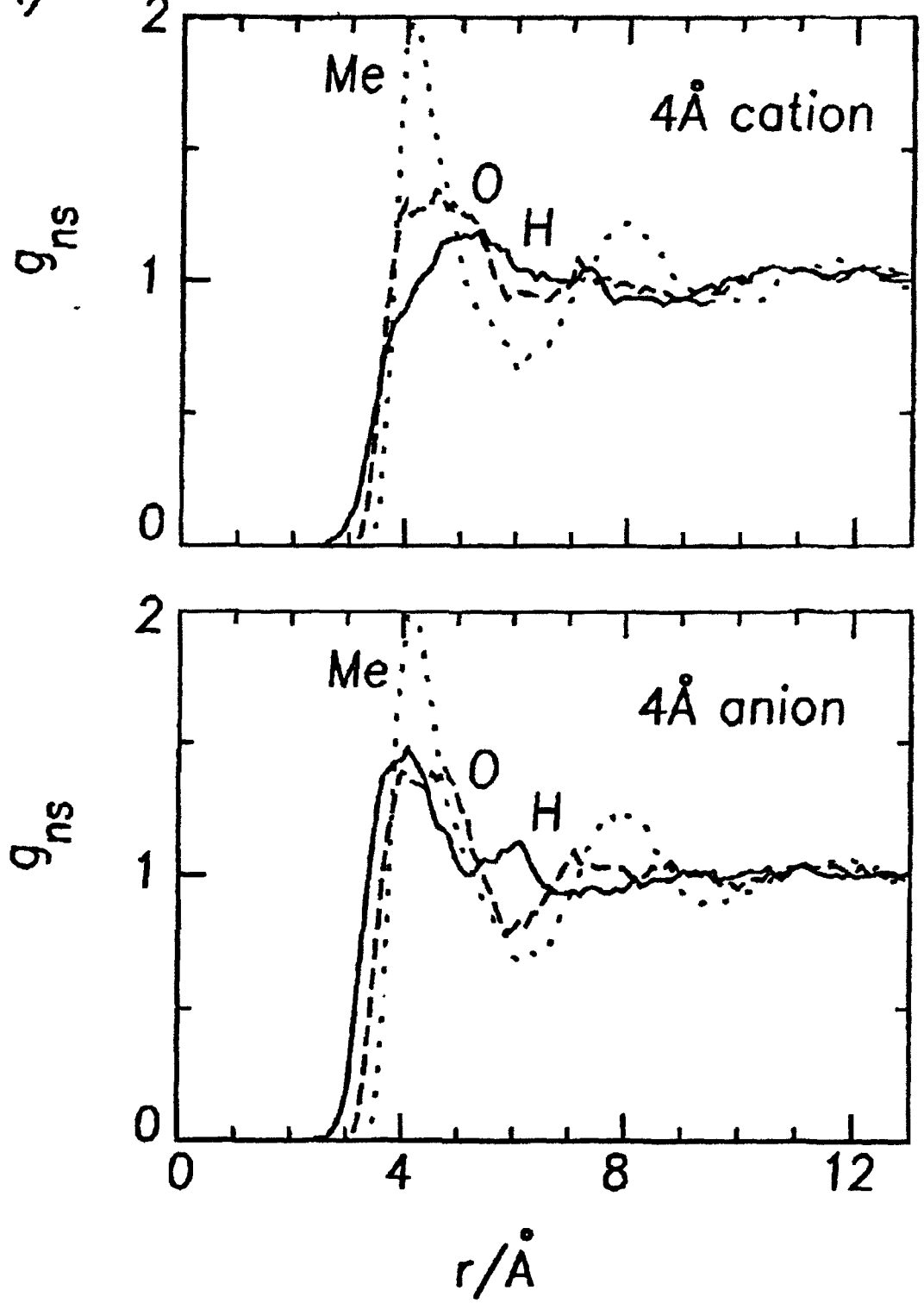

Fig. 3A

(B)

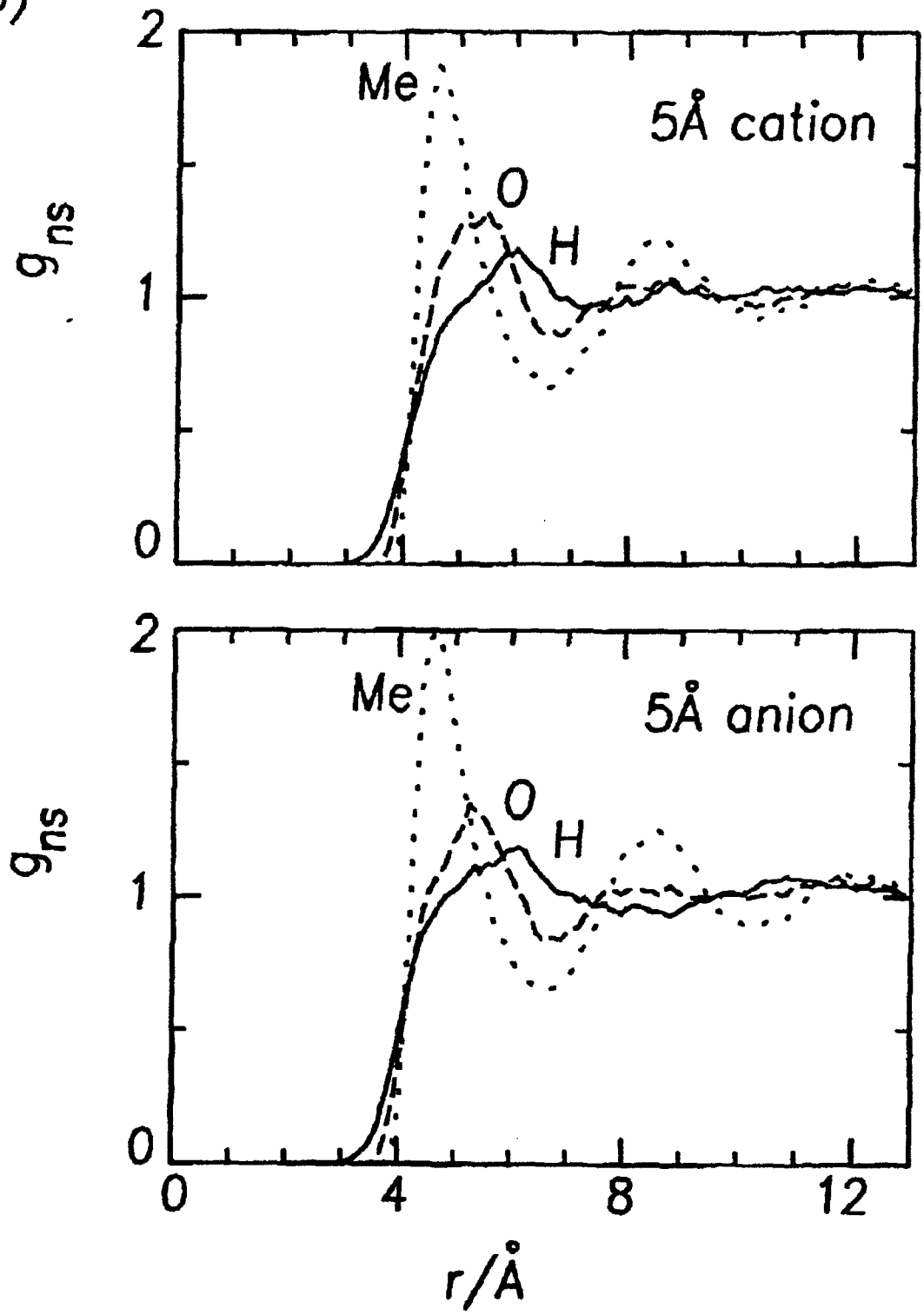

Fig. 3B

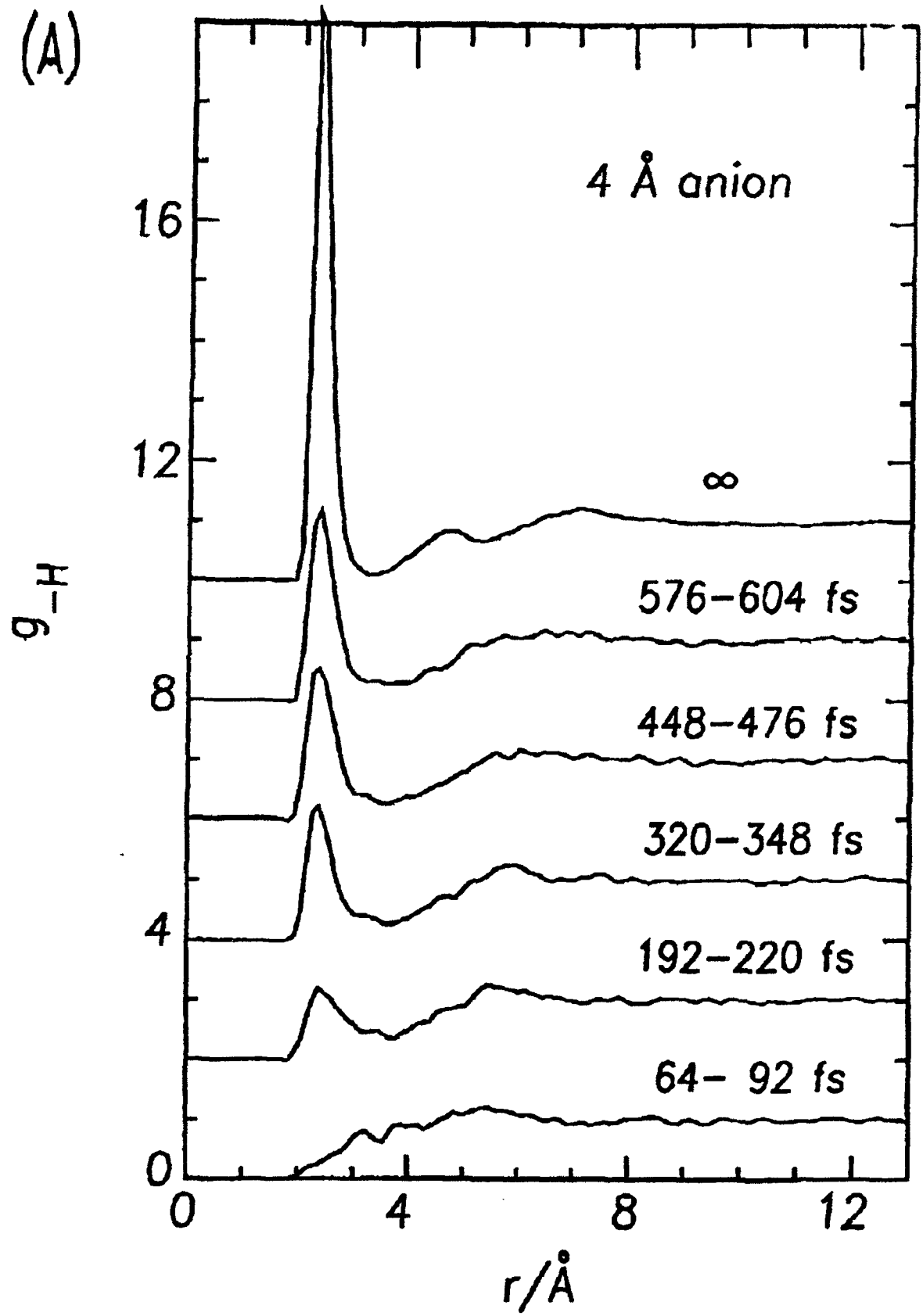
(A)
4 Å anion
16
12
8
4
0
∞
576–604 fs
448–476 fs
320–348 fs
192–220 fs
64– 92 fs
g_{H-O}
0
4
8
12
r/Å

1. 1. 44

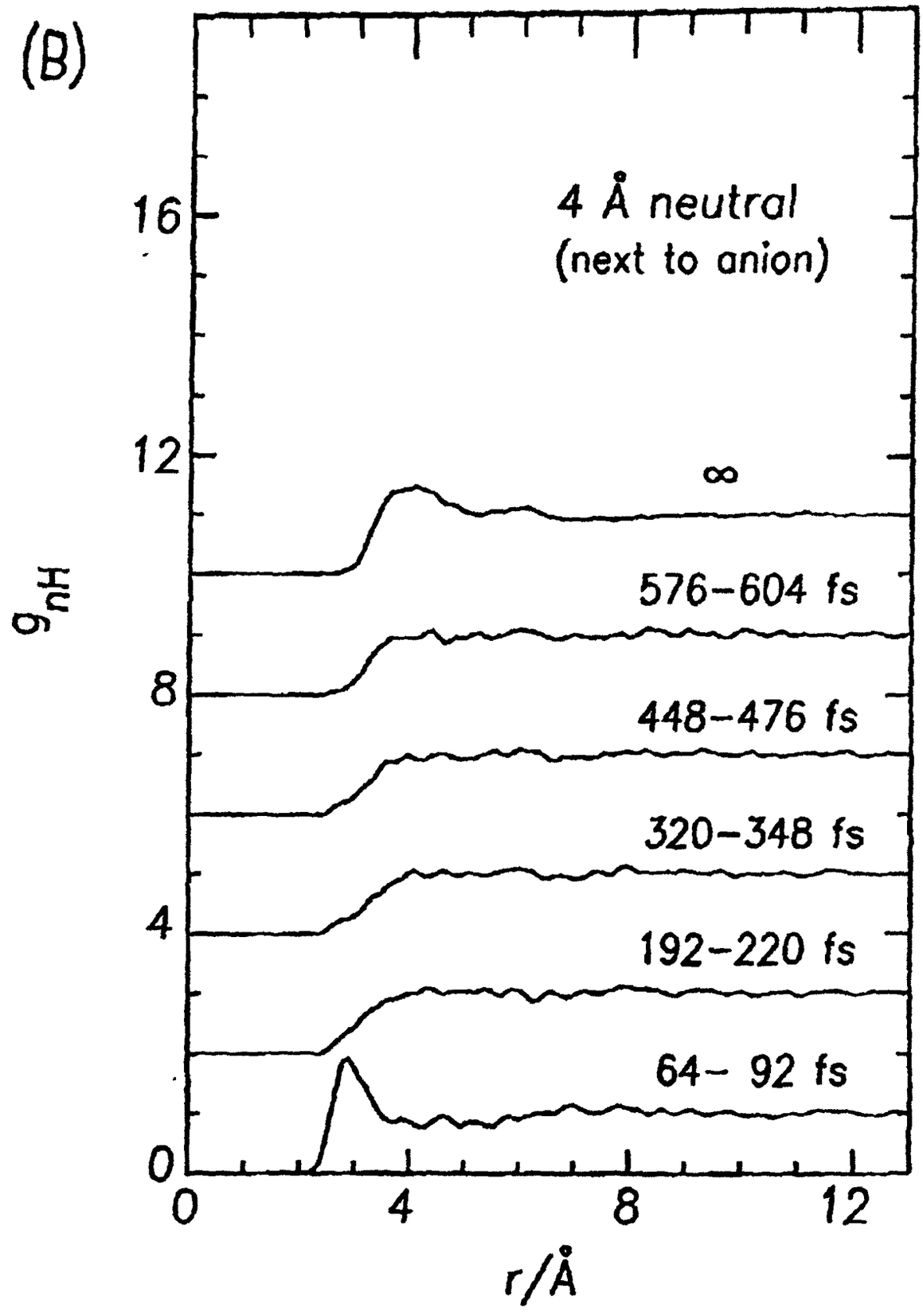
(B)
4 Å neutral
(next to anion)
∞
576–604 fs
448–476 fs
320–348 fs
192–220 fs
64– 92 fs
g_{nH}
0
4
8
12
16
0
4
8
12
r/Å

Fig. 4B

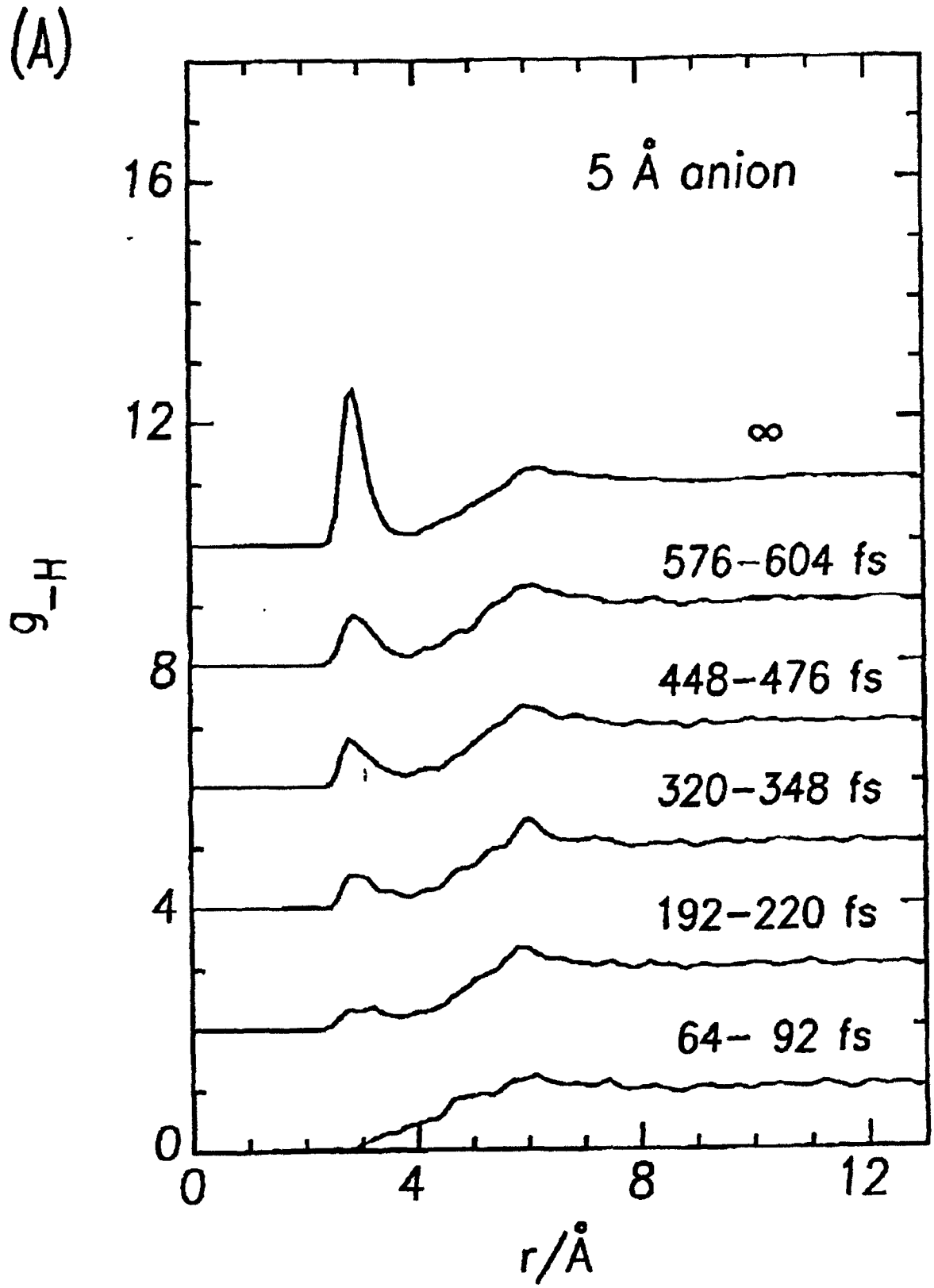
(A)
5 Å anion
16
12
8
4
0
∞
576–604 fs
448–476 fs
320–348 fs
192–220 fs
64– 92 fs
g_{I-H}
0
4
8
12
r/Å

Fig. 5A

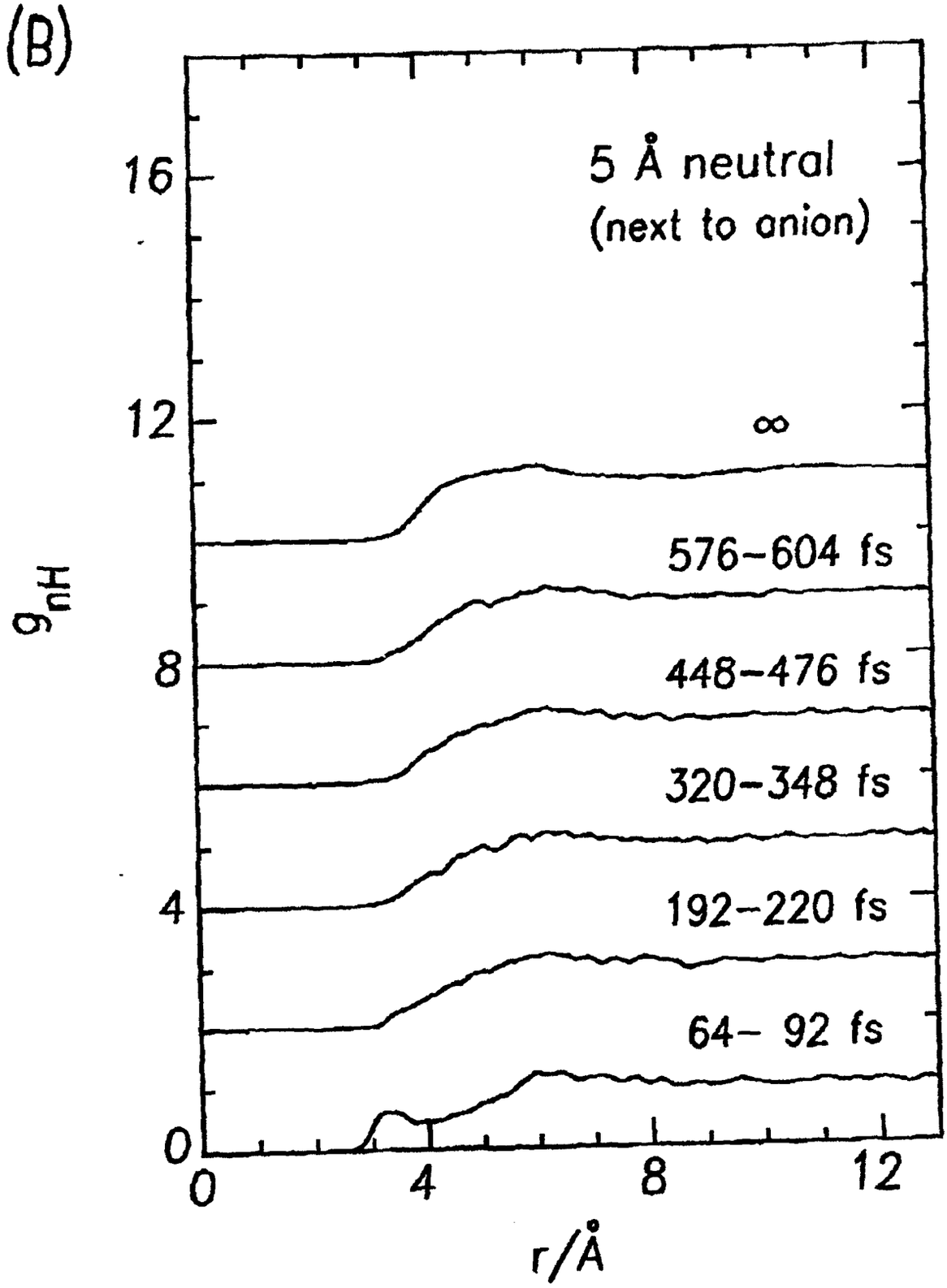
(B)
5 Å neutral
(next to anion)
∞
576–604 fs
448–476 fs
320–348 fs
192–220 fs
64– 92 fs
g_{nH}
16
12
8
4
0
0
4
8
12
r/Å

Fig. 5B

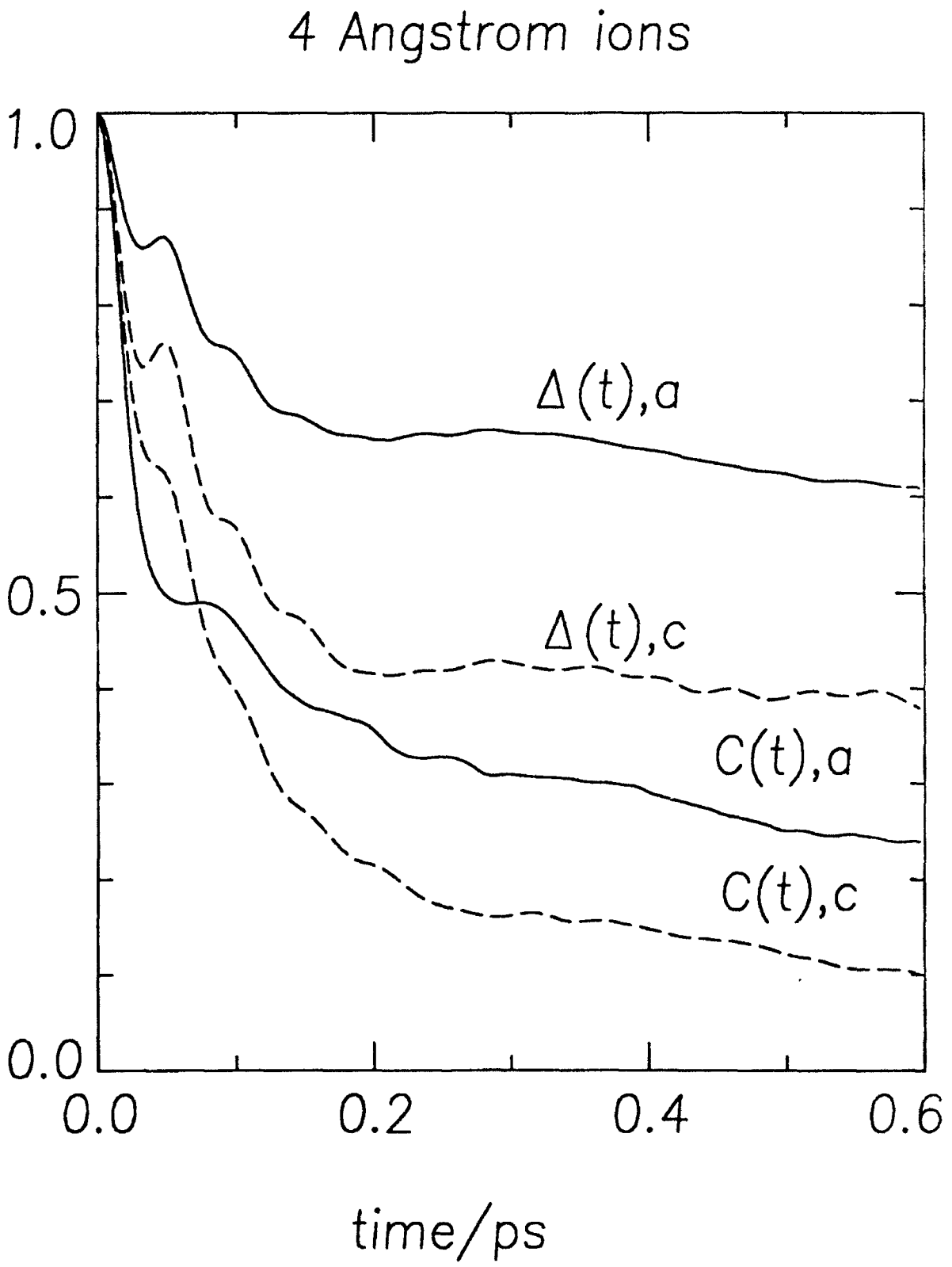

FIG 6

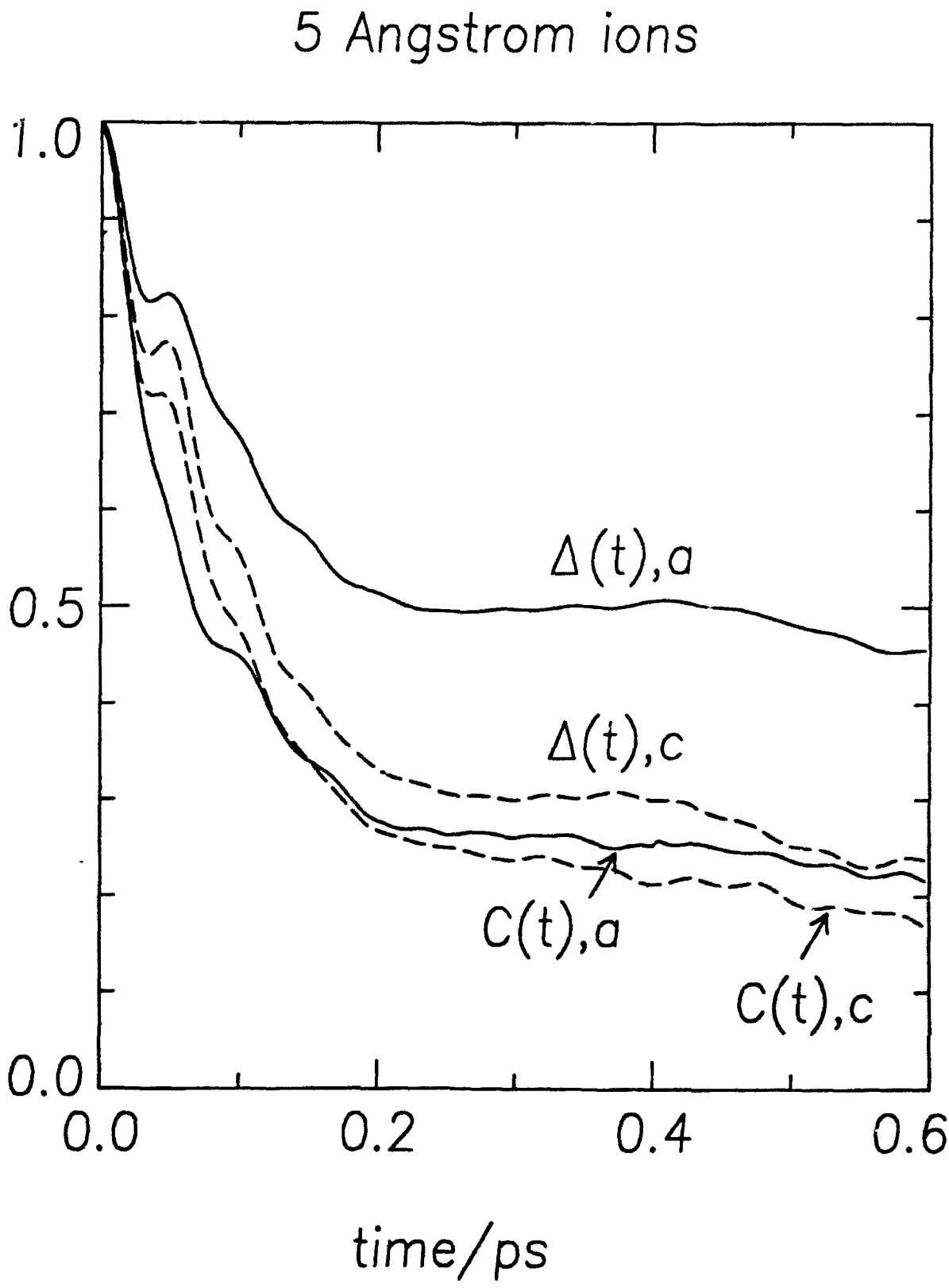

FIG 7